ACS ES&T Water

Open Access

This article is licensed under CC-BY-NC-ND 4.0

pubs.acs.org/estwater

Article

Gravity-Driven Membrane Filtration with Passive Hydraulic Fouling Control for Drinking Water Treatment: Demonstration of Long-Term Performance at Full Scale

Yixin Wei, Leili Abkar, Binura Senavirathna, Sara E. Beck, William Mohn, Matt Seitcher, and Pierre R. Bérubé*

Cite This: ACS EST Water 2025, 5, 70−80

Read Online

ACCESS | Metrics & More | Article Recommendations | Supporting Information

ABSTRACT: The present study evaluated the performance of a full-scale gravity-driven membrane filtration system with passive hydraulic fouling control (PGDMF) for drinking water treatment in a small community over a 3-year period. The PGDMF system consistently met the design flow and regulated water quality/performance parameters (i.e., total coliform, *Escherichia coli*, turbidity, and membrane integrity). The instantaneous temperature-corrected permeability (TCP) varied seasonally, being greater during the winter months. The overall TCP decreased slowly to ∼60% of the initial value by the end of 3 years, a TCP that is much greater than would have been expected without passive hydraulic fouling control. Although it was not possible to directly link the observed seasonal changes in TCP to potential seasonal changes in the biofilm microbiome, the analysis did suggest that the lower TCP during summer months was due to a greater microorganism richness in the feed and presence of filamentous, stalked, and biofilm-forming bacteria in the biofilm. Operation with higher trans-membrane pressure (i.e., ∼30 vs ∼20 mbar) and more frequent passive hydraulic fouling control (i.e., every 12 vs 24 h) enabled a greater flow to be sustained. The study demonstrated the long-term robustness and performance of GDMF with passive hydraulic fouling control for drinking water treatment.

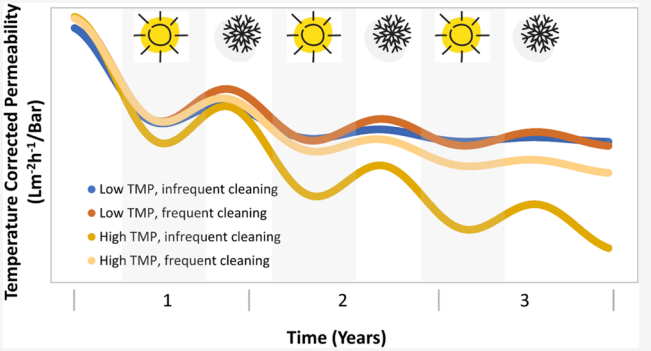

KEYWORDS: *biofilm, full-scale, long-term operation, gravity-driven membrane filtration, microbial community, passive hydraulic fouling control, seasonal variations, semicentralized water treatment*

1. INTRODUCTION

Gravity-driven membrane filtration (GDMF) uses hydrostatic pressure as the driving force for filtration and typically operates without any hydraulic or chemical cleaning measures, relying on the formation of a porous biofilm structure on the membrane surface to maintain a sustained permeate flux.[1−4] To enable the formation of a porous biofilm structure, the applied hydrostatic pressure (i.e., trans-membrane pressure, TMP) and the resulting permeate flux must be low.[1,2,4] By eliminating the need for complex mechanical and chemical systems, GDMF is considered as an ideal alternative to conventional drinking water treatment for small, remote, and/or marginalized communities.[4] The permeate flux in GDMF typically decreases by more than 90% at start-up.[1,5−7] Although a sustained permeate flux is eventually achieved, the large initial decrease translates to a significant reduction in the throughput capacity, potentially limiting the widespread adoption of GDMF.

A number of hydraulic cleaning approaches have been considered to increase the permeate flux of GDMF. Relaxation (i.e., permeate interruption) or backwash, on their own, were not reported to be very effective at increasing the permeate flux.[7−10] Contradicting results have been reported for air sparging, with some studies reporting limited impact of air sparging or crossflow,[8,9,11,12] while others reporting a beneficial impact on the permeate flux with low scouring intensity.[5,10] A higher scouring intensity can increase the density of biofilms, which could result in a lower permeate flux.[13] However, combing approaches used to release (i.e., relaxation and backwash) and scour (i.e., air sparging and crossflow) the biofilm were reported to substantively increase the sustained permeate flux.[5,9−11,14] Although effective at increasing the permeate flux, the implementation of the reported biofilm

Received: June 17, 2024
Revised: November 23, 2024
Accepted: November 25, 2024
Published: December 10, 2024

© 2024 The Authors. Published by American Chemical Society

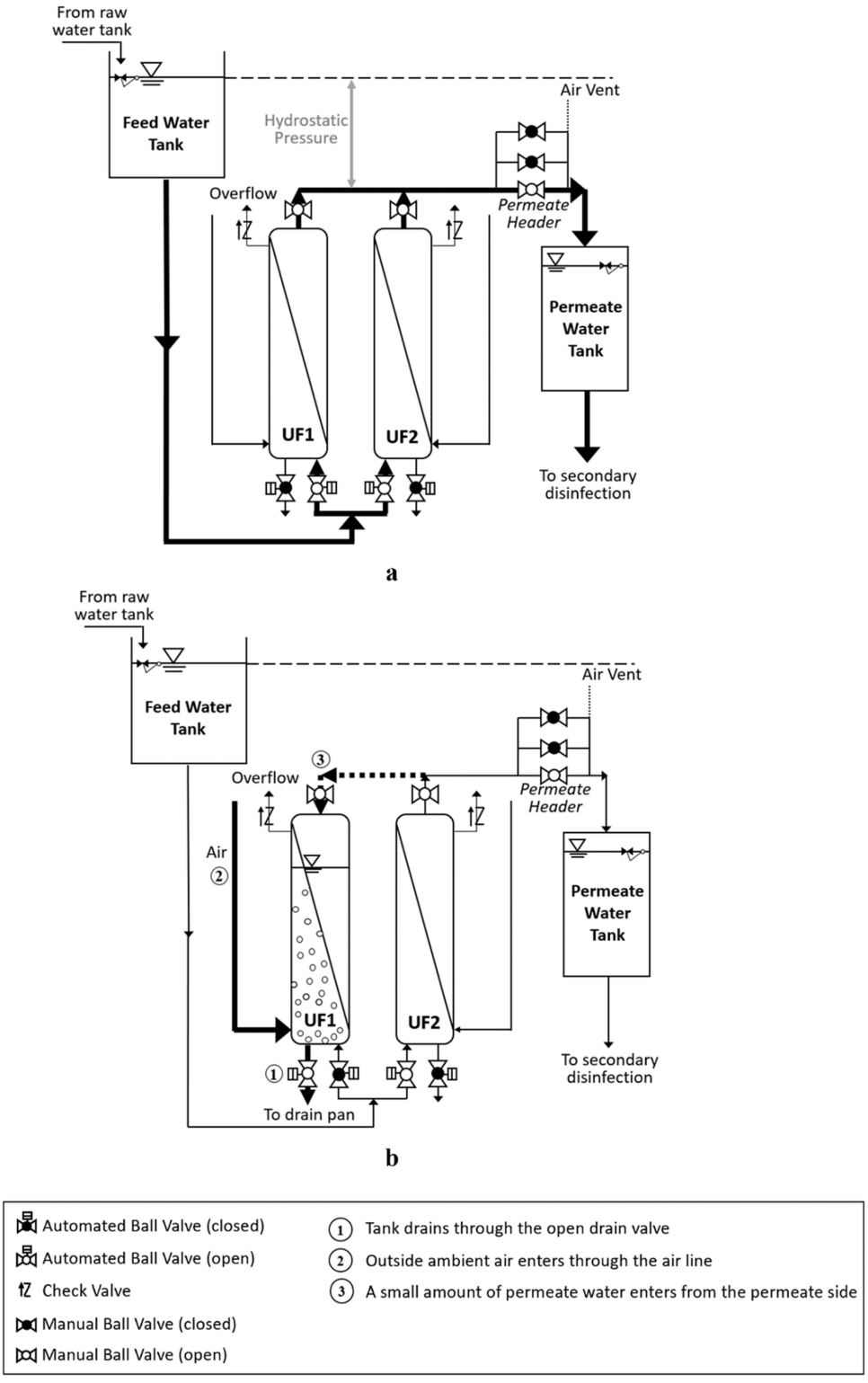

Figure 1. Schematic of Klehkoot PGDMF system ((a) dead-end filtration for both UF1 and UF2; (b) passive hydraulic cleaning for UF1 [dead-end filtration for UF2]; thick lines highlight process of interest [i.e., dead-end filtration or passive hydraulic cleaning]; Train A [UF1 and UF2] is illustrated, Train B [UF3 and UF4] is identical to Train A).

release and scouring approaches requires the use of mechanical systems (e.g., pumps and/or blowers), adding complexity and reducing the attractiveness of GDMF for use in small, remote, and/or marginalized communities.

Inspired by the mechanisms induced when a bottle of water is inverted, an alternative nonmechanical approach was developed to release and scour the biofilm.[15] Air, for sparging, can be drawn into a membrane module by the vacuum generated when the tank in which the module is housed is drained (Figure 1). The vacuum also provides the driving force for backwashing. Because air sparging and backwashing induced by the tank drain are generated without any complex

https://doi.org/10.1021/acsestwater.4c00553
ACS EST Water 2025, 5, 70−80

mechanical systems, we refer to these as passive hydraulic cleaning approaches, or passive gravity-driven membrane filtration (PGDMF) when applied to GDMF.

The efficacy of passive air sparging and backwash, combined with relaxation for hydraulic cleaning, was demonstrated with a pilot-scale PGDMF consisting of multiple custom and commercially available (ZeeWeed 1500, Veolia Water Technologies & Solutions, Oakville Canada) membrane modules.[16] The study confirmed that a greater permeate flux was achieved with, than without, passive hydraulic cleaning. Passive hydraulic cleaning also effectively prevented the accumulation of solids within the membrane modules, which occurred without hydraulic cleaning. Based on the performance of the pilot-scale PGDMF, and its promise as a simple approach to drinking water treatment, a full-scale PGDMF system was commissioned by Indigenous Services Canada and Nuu-Chah-Nulth Tribal Council to provide potable water for the Klehkoot Reserve of the Hupacasath First Nation on Vancouver Island in British Columbia, Canada.

Because PGDMF is a novel approach to drinking water treatment, the British Columbia First Nation Health Authority required the performance of the Klehkoot system to be validated, which is the main objective of the present study. Performance was quantified based on the ability to meet the design flow and regulatory water quality requirements. The study also provided an opportunity to assess seasonal variations and the impact of operational set-points, notably the trans-membrane pressure (TMP)[1,14,17−20] and the frequency of passive hydraulic cleaning, as these are expected to impact the performance of PGDMF and are the only two readily adjustable operational set-points at the Klehkoot PGDMF.

2. METHODS

2.1. Full-Scale PGDMF System Setup. *2.1.1. System Description.* The Klehkoot PGDMF system, which serves 10 households, consists of one raw water holding tank (capacity: 0.606 m^3) and two parallel PGDMF trains (each with two membrane modules: Train A (modules UF1 and UF2) and Train B (modules UF3 and UF4)), one permeate water tank (capacity: 0.397 m^3), one drain pan (capacity: 0.0265 m^3), and a secondary chlorine disinfection system (Figure 1). Each PGDMF train includes one feedwater tank (capacity: 0.114 m^3) and two PVDF hollow-fiber outside-in ultrafiltration membrane modules with a nominal pore size of 0.02 μm and a filtration area of 55.7 m^2 per module (ZeeWeed 1500, Veolia Water Technologies & Solutions, Oakville, Canada). ZeeWeed 1500-type membranes were selected because they are housed within an enclosed casing that can easily be configured to generate the vacuum required for passive hydraulic cleaning.[16] The hollow-fiber geometry and outside-in flow of the ZeeWeed 1500-type membrane modules have a high membrane packing density, resulting in a small system footprint, and unlike inside-out flow hollow fibers,[21] do not tend to clog.[16] The modular configuration of ZeeWeed 1500-type membrane modules also facilitates future expansion, if needed, without requiring extensive infrastructure upgrades.

Raw water is pumped from the Sproat River to the raw water holding tank, as needed to maintain a minimum liquid level, from which the raw water flows by gravity to the feedwater tank for each PGDMF train. The flow of raw water from the holding tank to the feedwater tank is controlled by a float valve, which maintains a constant liquid level (±2 cm) in the feed tank. From the feedwater tanks, the feedwater flows through a coarse strainer and then to the membrane modules, the permeate header, and the permeate tank. The water level in the permeate header is controlled by a manifold with three stacked pipes, each at a different elevation. The difference in water level between the feedwater tank and the permeate header provides the driving force (i.e., TMP) for filtration. The permeate in the permeate tank is pumped to the equalization tank (capacity: 138 m^3) when the liquid level in the permeate tank reaches the maximum set point; a 6% solution of hypochlorite is added to the permeate when pumped from the permeate tank to achieve a target chlorine residual of 0.2 mg·L^{-1} in the distribution network, a regulatory requirement.[22] The water level (meters) in the permeate water tank is recorded every minute by the Supervisory Control And Data Acquisition (SCADA) system, enabling the permeate flow and the daily treated volume to be calculated. Following secondary disinfection and equalization, the treated water flows by gravity into the distribution network for the Klehkoot Reserve.

The filtration sequence for the PGDMF consists of repeating cycles of dead-end filtration (Figure 1a) and passive hydraulic cleaning (Figure 1b). The repeating cycles are automated and controlled by the SCADA system. During dead-end filtration, the feedwater valve is open and the drain valve is closed. Feedwater flows by gravity from the feedwater tank to the membrane module. The permeate water from UF1 and UF2 is combined through a tee connection to the permeate header and flows by gravity to the permeate water tank. Passive hydraulic cleaning occurs after the dead-end of the filtration period. During passive hydraulic cleaning, the feedwater valve is closed. Passive hydraulic cleaning consists of a relaxation (i.e., permeate flux interruption) period of 55 min during which the drain valve is closed, followed by 5 min of module (i.e., membrane tank) drain during which the drain valve is open. Passive air sparging and backwashing occur during the tank drain. A ∼1 h relaxation period followed by a few minutes of air sparging was identified by Oka et al.[5] as optimal when coupled with air sparging. The average air sparging flow is 9 L min^{-1} and the total volume of air added for sparging per drain is approximately 18 L; equivalent to the drain volume of the ZeeWeed 1500 membrane modules. The bulk of the liquid in the module drains in approximately 2 min; only backwash water drains for the remaining 3 min. No air for sparging enters the module once the bulk module drain is completed. Only one membrane module undergoes passive hydraulic cleaning at a given time. The check valve on the vent pipe enables air to escape from the module when filled with feedwater at the start of a dead-end filtration cycle and prevents air from entering the module when drained. Reject and backwash water flows by gravity to the drain pan and, subsequently, to an infiltration well. Excess production flow beyond the demand or treated water reservoir capacity is discharged to an infiltration well. A comprehensive cost analysis was not within the scope of this study; nonetheless, the implementation of the system at Klehkoot enabled the capital costs of PGDMF to be accurately obtained for a community of that size. For the system components described above, excluding the secondary disinfection (i.e., chlorination system), the capital cost was $36,000 USD. Approximately 1/3 of this cost was for the membrane modules, 1/4 for the system tanks, piping, and valves, and 1/4 for the SCADA system.

2.2. Stages of the Study and Operational Set-Points. A summary of the stages and operational set-points is

https://doi.org/10.1021/acsestwater.4c00553
ACS EST Water 2025, 5, 70−80

presented in Table 1. Low TMPs, in the range considered, have been reported by others as ideal in limiting reduction in permeability.[1,14,17−20] The upper limit of the TMP range was constrained by the geometry of the Klehkoot PGDMF and the prefabricated building in which it was housed. A passive hydraulic cleaning frequency of once per 24 h was selected based on the results from Oka et al.,[5] while a frequency of once per 12 h was considered should more extensive hydraulic cleaning be required.

Table 1. Summary of Stages and Operational Set-Points

	stage 1		stage 2	
module	cleaning frequency[a]	TMP[c]	cleaning frequency[b]	TMP[c]
UF1	every 24 h	32 ± 0.5 cm	every 12 h	22 ± 0.5 cm
UF2	every 24 h	32 ± 0.5 cm	every 24 h	22 ± 0.5 cm
UF3	every 24 h	31 ± 2 cm	every 24 h	31 ± 2 cm
UF4	offline	offline	every 12 h	31 ± 2 cm

[a]23 h dead-end filtration followed by passive hydraulic cleaning. [b]11 h dead-end filtration followed by passive hydraulic cleaning. [c]Difference in TMP between UF1, UF2 and UF3, UF4 due to slight geometry variances.

During Stage 1, which lasted approximately 3 months, UF1, UF2, and UF3 were operated in parallel, all with similar operational set-points. At the beginning of Stage 2, which is ongoing and for which 33 months of operational data are presented, the operational set-points of UF1 and UF2 were modified (Table 1) while those of UF3 remained unchanged. UF4 was also started at the beginning of Stage 2. The original UF3 (UF3a) was removed and replaced with a new membrane module (UF3b) approximately 18 months after the start of Stage 2. Membrane fibers were harvested from UF3a when removed for microbiome analysis (Section 2.3.2).

2.3. System Monitoring and Analytical Methods. *2.3.1. Water Quality Parameters.* Water temperature and turbidity levels were measured on-site by the plant operator twice a week. The temperature of the permeate was measured with a thermometer and assumed to be the same as that of the feed and in the membrane modules. The turbidity of the feed and permeate was measured using a HACH 2100Q Potable Turbidimeter, calibrated as outlined in the HACH documentation (Single step RapidCal for Low-Level Regulatory Reporting from 0−40 NTU (FNU)). Samples of the feed, permeate, and reject water for total organic carbon (TOC), dissolved organic carbon (DOC), ultraviolet absorbance at 254 nm (UVA), specific UVA (SUVA), total suspended solids (TSS), total phosphorus (TP), ammonia, and Total Kjeldahl Nitrogen (TKN) analysis were collected on-site by the plant operator and transported to laboratory at the University of British Columbia (Vancouver, Canada). All samples were refrigerated at 4 °C in the dark during storage and transportation. Sample collection was performed twice a week during the summer months in Year 1 of Stage 2 and every 4−6 weeks for the remainder of the study period. TOC and DOC were measured with a TOC analyzer (TOC-L CPH PC-controlled high-sensitivity model with Autosampler ASL from Shimadzu) using Non-Purgeable Organic Carbon (NPOC) method (5310 B in APHA Standard Methods).[23] DOC was measured after filtration through a 0.45 μm filter (Supor poly(ether sulfone) Membrane from Pall Corporation). UVA was measured immediately after filtration through a 0.45 μm filter (same as DOC) and was analyzed with a Spectronic Unicam UV-300 UV−visible spectrometer (5910 B in APHA Standard Methods).[23] SUVA was calculated as the ratio of UVA to DOC (×100). TSS was measured after filtration through glass fiber filters (G4 Circles Fisherbrand) with the residuals oven-dried at 105 °C for ∼12 h. TP was measured after sample digestion (4500-P B in APHA Standard Methods)[23] and was analyzed using a PerkinElmer Optima 7300 DV Series Coupled Plasma Optical Emission Spectrometry Systems at the wavelength of 213.617 and 214.914 nm. Ammonia was measured with a Lachat Quikchem 8500 Series 2 Flow Injection Analysis System using Flow Injection Analysis method (4500-NH3 H in APHA Standard Methods).[23] TKN was measured after sample digestion (same as TP) and was analyzed with Block Digestion and Flow Injection Analysis method using the same apparatus as Ammonia (4500-Norg D in APHA Standard Methods).[23] Measured values that were not within 2 standard deviations (S.D.) from the average value of the given period were considered outliers and excluded from the analysis (<10% of measurements were excluded).

Total coliform, *Escherichia coli*, and free chlorine residual measurements were managed independently from the present study by the First Nation Health Authority (FNHA); measurements were downloaded from the FNHA Compliance 365 Database. Total coliform and *E. coli* were measured using IDEXX Colilert tests (9223B in APHA Standard Methods).[23] Free chlorine residual was measured using a HACH DR300 Pocket Mid-Range Chlorine Colorimeter, calibrated, and analyzed with the US EPA DPD Method 10245 (4500-Cl G in APHA Standard Methods).[23] Reported free chlorine measurements are for the furthest location in the water distribution network for the Klehkoot Reserve.

2.3.2. Microbiome Analysis. Samples of the feed, reject, and permeate were collected monthly for DNA extraction for an 18-month period during the latter half of Stage 2. The biofilm of the Klehkoot PGDMF cannot be readily accessed without sacrificing modules; for this reason, biofilm samples for DNA extraction were only collected on one occasion from membrane fibers of module UF3a when removed from operation (Section 2.2). Biofilm samples were collected randomly from selected hollow fibers at the top, middle, and bottom sections of the membrane (Supporting Information, Figure S1).

DNA extraction and 16S rRNA sequencing were performed as outlined in Abkar et al.[24] Extracted DNA samples were shipped to Microbiome Insights, Inc. for sequencing. The raw sequencing data was demultiplexed with primers removed as recommended by Langille Lab,[25] using QIIME2.2023.2 software. Raw data were evaluated for their sequencing quality using FASTQC and MULTIQC. The Divisive Amplicon Denoising Algorithm 2 software package was used to remove errors and chimeras introduced during the sequencing. Low frequency and rare operational taxonomic units (OTUs) were filtered out based on ≤0.1% of the mean frequency of all of the OTUs. The rarefaction curves were generated after running the sequences through the multiple sequence alignment program using fast Fourier transform, MAFFT (Supporting Information, Figure S2). The taxonomy was assigned based on the SILVA database (version 138 99% OTUs from 515F/806R region of sequences).[26] Microbiome diversity analysis was conducted using "diversity core- metrics-phylogenetic" software packages. The results were transferred to R Studio for further analysis and visualization. β diversity was measured by

https://doi.org/10.1021/acsestwater.4c00553
ACS EST Water 2025, 5, 70−80

the weighted unique fraction (Uni-Frac) (Supporting Information, Figure S2) and Bray−Curtis.

2.3.3. Hydraulic Parameters. Membrane integrity testing was conducted on a weekly to monthly basis and quantified using pressure decay tests.[27]

Total permeate flow (Q) of all operating modules was calculated by multiplying the water level change per minute in the permeate water tank by the cross-sectional area of the permeate water tank. The permeate flow for a module was calculated as the difference between the average total permeate flow, measured approximately 60 min before and after passive hydraulic cleaning for that module, and the total permeate flow during passive hydraulic cleaning for that module. Permeate flux was calculated using eq 1, where J is the permeate flux (L m^{-2} h^{-1}) measured at a temperature T (°C), Q is the permeate flow (m^3 day^{-1}), and A is the membrane surface area generating the permeating flow (m^2). The temperature-corrected (i.e., to 20 °C) permeability (TCP) was calculated using eq 2 (L m^{-2} h^{-1}/bar),[27] T_{20} is 20 °C, and TMP is the trans-membrane pressure (bar).

$$J_T = \frac{Q}{A} \tag{1}$$

$$\begin{aligned} \mathrm{TCP} = (J_T \times \{&[1.784 - (0.0575 \times T) + (0.0011 \times T^2) \\ &- (10^{-5} \times T^3)]/[1.784 - (0.0575 \times T_{20}) \\ &+ (0.0011 \times {T_{20}}^2) - (10^{-5} \times {T_{20}}^3)]\})/\mathrm{TMP} \end{aligned} \tag{2}$$

Note that no hydraulic data was recorded for approximately 50 days during the fall of 2022 due to a fault in the data logging function of the SCADA system.

2.4. Data Interpretation. Summative parameters were extracted from the time-series TCP data by fitting relevant models using the Monte Carlo Algorithm of ProFit (version 7.1.8). χ^2 analysis was used to assess the goodness of fit. For the modeling results, the estimated parameters and the associated standard errors are reported. For the water quality monitoring results, the average values and standard deviations are reported. All comparisons, statistical tests, data modeling, and reporting were based on a 95% confidence interval.

2.5. Raw Water. The monitored characteristics of the raw source water (i.e., the Sproat River) during the study period are summarized in Table 2.

Note that some raw water characteristics, notably the organic and nutrient content, have been reported to impact the performance of lab-scale GDMF;[4] therefore, it is reasonable to expect that the performance of PGDMF could also be impacted by these, and potentially other, raw water characteristics. Ongoing research, beyond the scope of the present study is investigating the impact of different, and seasonally variable, source water characteristics on the performance of PGDMF.

Table 2. Raw Water Characteristics

parameter	unit	average ± S.D.	range [min, max]
turbidity	NTU	0.33 ± 0.11	[0.15, 0.82]
temperature	°C deg	12.7 ± 5.9	[3.9, 22.7]
total organic carbon	mg L^{-1}	0.93 ± 0.23	[0.67, 1.57]
dissolved organic carbon	mg L^{-1}	0.80 ± 0.22	[0.55, 1.46]
ultraviolet absorbance at 254 nm	cm^{-1}	0.019 ± 0.007	[0.008, 0.034]
specific UVA	L mg^{-1} m^{-1}	2.46 ± 0.57	[1.18, 4.01]
total suspended solid	mg L^{-1}	0.85 ± 0.30	[0.30, 1.29]
total phosphorus	mg L^{-1}	0.39 ± 0.12	[0.17, 0.63]
ammonia	mg L^{-1}	0.19 ± 0.15	[0.04, 0.52]
total kjeldahl nitrogen	mg L^{-1}	3.68 ± 2.11	[1.1, 7.2]
total coliform	MPN	25.7 ± 25.8	[<1, >200]
E. coli	MPN	3.05 ± 3.38	[<1, 12.4]

3. RESULTS AND DISCUSSION

3.1. Validation of Performance of the Klehkoot PGDMF System. The overall performance of the Klehkoot PGDMF system was assessed based on the ability to meet design production flow and regulatory water quality requirements.

The design production flow for the Klehkoot PGDMF was 10 m^3/day, a requirement of the Hupacasath First Nation to meet the current water demand for the Klehkoot Reserve. The actual production flow for the different modules during this study is illustrated in Figure 2. Regardless of the number of membrane modules in operation (Section 2.2), seasonal variations (Section 3.2), and operational set-points (Section 3.3), the design production flow was consistently met, with the actual production flow ranging from 20 to 40 m^3/day during the study period (i.e., first 3 years of operation). Note that the production flow in excess of demand is discharged to an infiltration ditch. As discussed in Section 3.3, the Klehkoot PGDMF system is expected to meet the design production flow for a number of years to come (predictions for the second 3 years of operation are presented in Figure 2).

The regulatory water quality requirements[22,28] for the Klehkoot PGDMF system are listed in Table 3. Also listed in Table 3 is a summary of the treated water quality monitored during the present study. Regulatory requirements for total coliform, *E. coli*, turbidity, and membrane integrity were consistently met. Residual-free chlorine concentrations were on average lower than the target value; this is because the initial residual chlorine concentration was set to 0.05 mg/L, at the requests of FNHA and residents of the Klehkoot Reserve, and was progressively increased during year 2 of the study to be consistently greater than 0.2 mg/L.

3.2. Impact of Seasonal Variations. Although knowledge of the production flow is essential to assess the ability to meet demand flow, it provides limited insight into performance. This is because production flow can be substantially impacted by raw water viscosity (which is largely governed by temperature, which changes seasonally), as well as operational set-points (e.g., TMP, and the number of modules in operation) depending on operational goals. For this reason, TCP (temperature-corrected permeability), which normalizes the production flow with respect to the impact of temperature on viscosity, TMP, and membrane surface area, was used as a more informative metric of performance. TCP for different modules is presented in Figure 3.

The progression of TCP observed in the present study differs from that reported in studies by others for GDMF. Typically, TCP is characterized by a rapid (within a few days to a few weeks) decline to a relatively sustained but low value, typically $\lesssim$10% of the initial value.[1,2,4,7,8,20,29−31] In contrast, throughout the present study, TCP consistently remained $\gtrsim$25, $\gtrsim$35, and $\gtrsim$45% of its initial value for UF4, UF3, and UF2, as well as UF1, respectively. At the end of the study period, once fluctuations had dampened (Section 3), TCP for all modules was $\gtrsim$45% of its initial value. These results demonstrate the

https://doi.org/10.1021/acsestwater.4c00553
ACS EST Water 2025, 5, 70−80

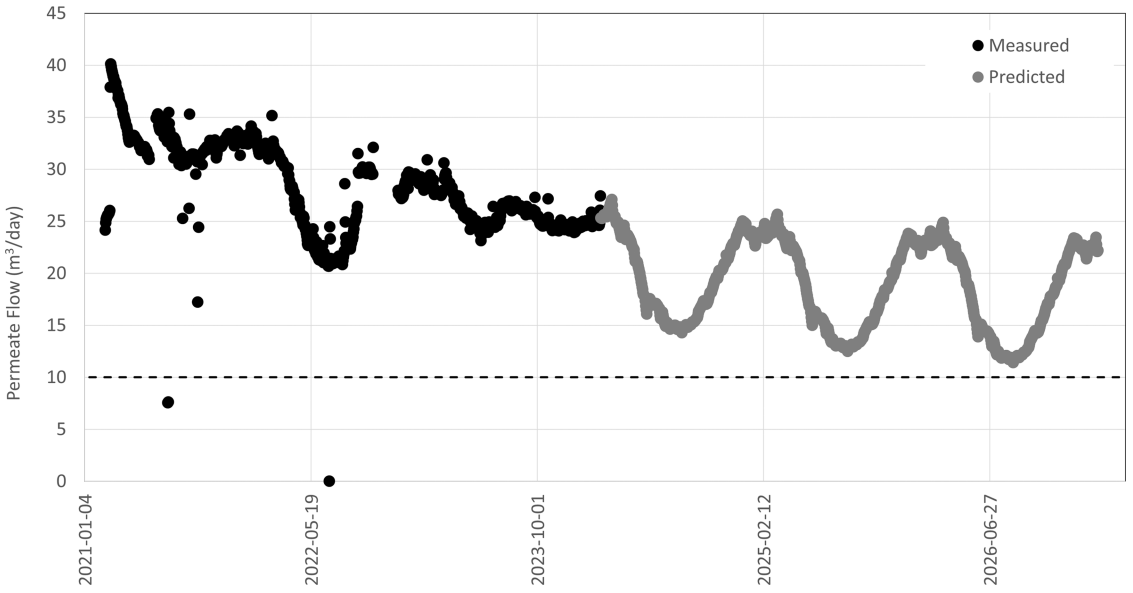

Figure 2. Measured and predicted production flow. The horizontal dotted line corresponds to minimum design production flow; data for 6 calendar years are presented: 3 years of measured flow and 3 years of predicted flow; predicted flow assumes all 4 membrane modules are online and operating with a high TMP (0.32 mbar) and frequent hydraulic cleaning (every 12 h), the temperature-corrected permeability can be estimated with eq 2, and the temperature variations observed during the 3 years of the study (Figure 3) repeat in the second 3 years.

Table 3. Regulated Water Quality Parameters

parameter	unit	target value[a]	measured value[b]	range [min, max]
total coliform[b]	MPN·100 mL^{-1}	0.0	<1[c]	
E. coli	MPN·100 mL^{-1}	0.0	<1[c]	
free chlorine residual	mg L^{-1}	>0.2	0.18 ± 0.13	[0.01, 0.96]
turbidity	NTU	<0.1	0.10 ± 0.08	[0.03, 0.80]
membrane integrity	LRV	>3	>5.5[d]	

[a]Based on the most stringent of Protocols for Centralized Drinking Water Systems in First Nations Communities[22] and Guidelines for Canadian Drinking Water Quality.[28] [b]Values correspond to average ± standard deviation. [c]Minimum detection limits, for the method used. [d]Maximum detection limits, for the method used.

effectiveness of passive hydraulic cleaning in maintaining a higher permeability.

During Stage 1, the three operating modules (UF1, UF2, and UF3) that had similar operational set-points for TMP and passive hydraulic cleaning frequency (Table 1) also had similar TCPs. At the start of Stage 2, in which the operational set-points were modified for UF1 and UF2, TCP continued to decline at a rate similar to that in Stage 1, regardless of the operational set-points. However, as Stage 2 progressed, alternating periods of decreases and increases in TCP were observed.

Raw water characteristics can change seasonally; and therefore, could generate the observed seasonal variable trends in TCP, as suggested by Lee et al.[32] The DOC[1,2,32] and phosphorus[18,33] concentrations of the raw water have been reported to substantively impact the biofilm permeability in GDMF. However, the DOC and total phosphorus concentrations in the raw water remained relatively stable throughout the present study (Table 2), with no consistent or significant seasonal trends (results not presented). Therefore, it is unlikely that changes in DOC and/or phosphorus concentrations of the raw water were predominantly responsible for the observed seasonal trends in TCP.

Raw water temperature changes can also impact the biofilm permeability in GDMF; however, inconsistent results have been reported by others, with some studies indicating that greater temperatures have a negative impact,[34] no impact,[35] or a positive impact.[36] Raw water temperature variation has also been reported to impact the composition, activity, and products of the microbial communities in wastewater treatment systems,[37,38] affecting fouling in membrane bioreactors[39] and tertiary membrane systems.[38] Recurring seasonal variations in temperature were suggested to generate seasonal variations in the composition of microbial communities.[37,40] In the present study, the feedwater temperature varied substantively throughout the year, ranging from 4 °C in winter to 22.7 °C in summer (Figure 3). In general, periods of elevated temperature coincided with periods of low TCP, while periods of low temperature coincided with periods of high TCP, indicating the negative impact of temperature. These results suggest that seasonal temperature variations and their impact on the biofilm microbial community could be responsible for the observed periods of peaks and valleys in TCP, which repeated in the first two years. These results align with other studies which concluded that variations in temperature have a greater impact on microbial communities than variations in other raw water characteristics (e.g., DOC, phosphorus).[37,40]

A microbiome analysis of the biofilm (i.e., sampled from UF3a) in summer (i.e., August 2022), indicated that putative filamentous, stalked, biofilm and extracellular polymeric substance (EPS) forming bacteria were predominant (Supporting Information, Figures S3 and S4). These bacteria would be expected to form a dense biofilm with a low TCP.[41,42] Unfortunately, it was not possible to identify potential seasonal changes in the biofilm microbial communities that could impact TCP due to a lack of repeated biofilm microbiome analyses during different seasons (see Section 2.3.2).

The microbial communities in the feed and reject were originally considered as potential surrogates for those in the

https://doi.org/10.1021/acsestwater.4c00553
ACS EST Water 2025, 5, 70−80

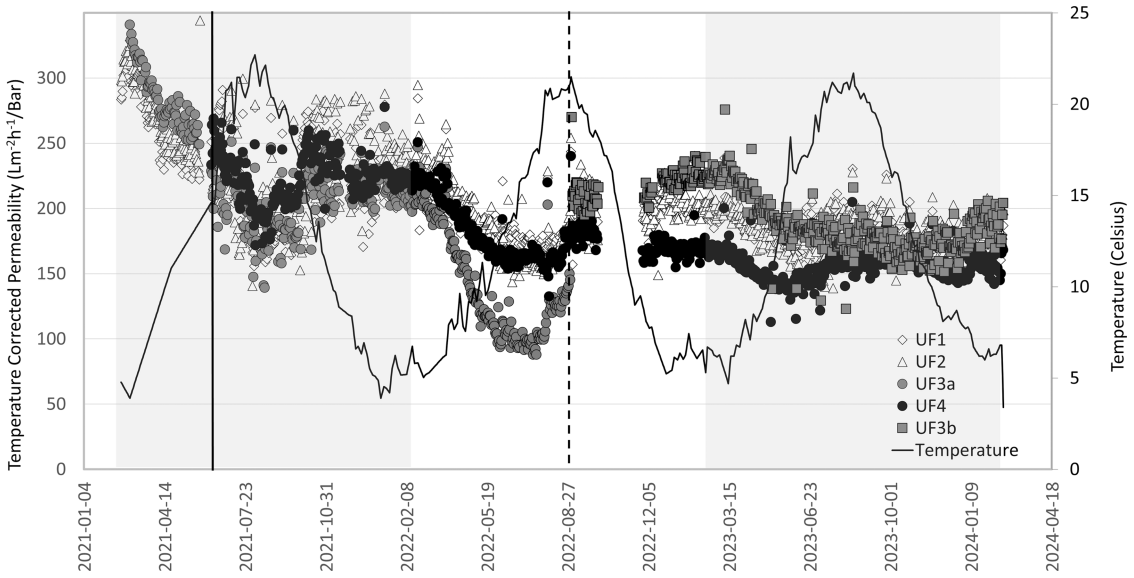

Figure 3. Temperature-corrected permeability varied by seasonal changes (mainly indicated by temperature changes). The solid vertical line denotes transition between Stage 1 and Stage 2; the dotted vertical line denotes when UF3a was removed/replaced by UF3b; successive calendar years are highlighted by alternating clear and shaded areas.

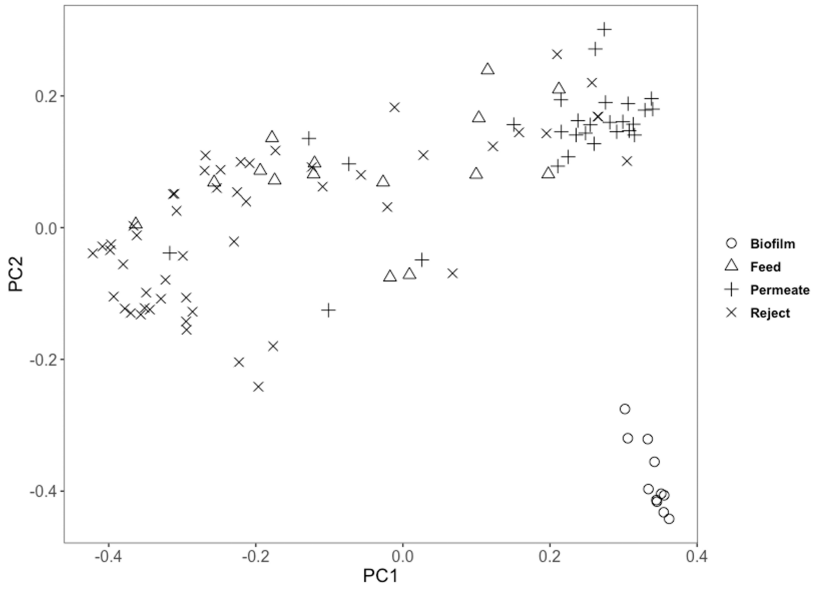

Figure 4. Similarity of composition between feed, reject, permeate, and biofilm communities depicted by principal component analysis of Bray–Curtis distance analysis. Results for feed, reject, and permeate are replicate measurements of ~monthly sampling events over an 18-month period; results for biofilm are replicate measurements of a single sampling event; and the corresponding scree plot is presented in Supporting Information, Figure S5.

biofilm. However, a β diversity analysis using Bray–Curtis (Figure 4) and Weighted Uni-Frac (Supporting Information, Figure S6) distance matrices indicated that the composition of the microbial communities in the biofilm was distinct from those in the feed and reject (Figure 4). This distinction was confirmed by PERMANOVA analysis (P value = 0.002). The distinct composition of the communities in the biofilm likely resulted from the selective retention of bacteria from the feed and adaptation of retained bacteria to environmental factors.[43−45] Further research is required to assess if seasonal changes in the biofilm microbial communities could be responsible for the observed yearly trends in TCP. The microbiome analysis of the feed (Supporting Information, Table S1) did, however, indicate a greater richness of bacteria (measured as OTUs) in summer than in winter, which could also have contributed to the formation of a thicker biofilm with a lower TCP in the summer than the winter.

The absence of repeating yearly peaks and valleys in TCP in studies by others is likely because most of these studies were conducted under controlled laboratory conditions with constant temperature and/or feed waters. As a result, the microbial communities in these previous studies likely did not substantially change with time. In addition, most previous published studies were conducted over relatively short periods (i.e., $\lesssim$100 days), during which substantive seasonal changes in raw water characteristics were not expected.

3.3. Impact of Operational Set-Points on the Temperature-Corrected Permeability. The evolution in TCP over

https://doi.org/10.1021/acsestwater.4c00553
ACS EST Water 2025, 5, 70−80

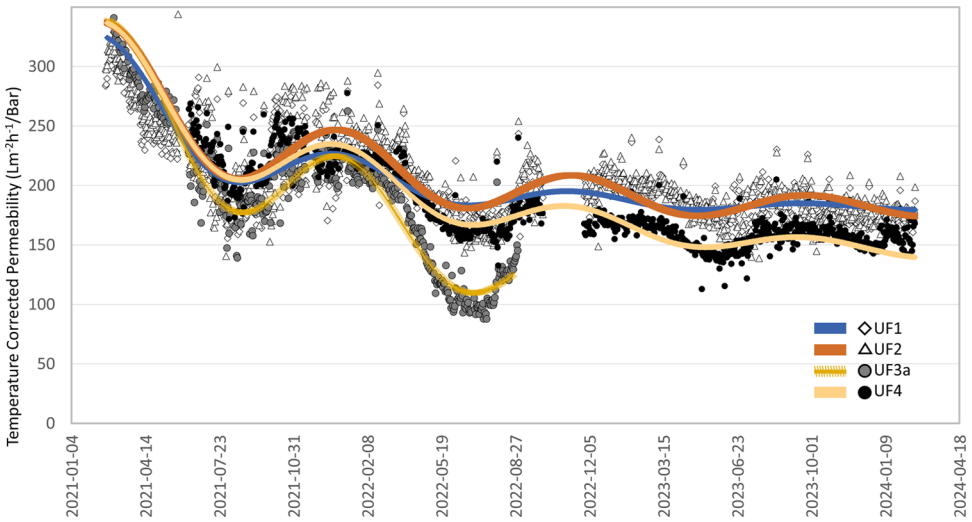

Figure 5. Sinusoidal model fitted to the temperature-corrected permeability.

Table 4. Summary of Rates of Decline in the Amplitude and Magnitude of Temperature-Corrected Permeability

	operation		summative parameter			
module	TMP [mbar]	cleaning frequency [h]	k_{Amp} [L m^{-2} h^{-1} bar^{-1} day^{-1}]	k_{TCP} [L m^{-2} h^{-1} bar^{-1} day^{-1}]	TCP_S [L m^{-2} h^{-1} bar^{-1}]	χ^2
UF1	22	12	0.0014 ± 0.003[a]	0.003 ± 0.0003[a]	172 ± 2.0[a]	3.49 × 10^5
UF2	22	24				4.50 × 10^5
UF4	31	12		0.0015 ± 0.0002[a]	138 ± 1.2[b]	1.63 × 10^5
UF3a	31	24	0.00054 ± 0.0006[b]		56 ± 1.9[b]	1.39 × 10^5

[a]± Corresponds to the (maximum − minimum)/2 for the estimated parameters. [b]± Vorresponds to the standard error of the estimated parameter.

time could be described by a sinusoidal relationship with exponentially decreasing overall value and amplitude of the sinusoidal relationship and a 1-year return period, as outlined in eq 3. An exponential decrease in the overall TCP to an expected sustained value is consistent with results from most GDMF studies by others.[1,2,4,7,8,20,29−31]

$$TCP_t = Amp(\exp^{-k_{Amp}t})Sin(t') + (TCP_I - TCP_S)\exp^{k_{TCP}t} + TCP_S \quad (3)$$

where TCP_t is TCP at time t (L m^{-2} h^{-1} bar^{-1}), t is time (days), TCP_I is the initial TCP (L m^{-2} h^{-1} bar^{-1}), and TCP_S is the expected TCP that can be sustained over a relatively long period (L m^{-2} h^{-1} bar^{-1}), Amp is the amplitude of the sinusoidal relationship (L m^{-2} h^{-1} bar^{-1}), k_{TCP} and k_{Amp} are the rates of decline (L m^{-2} h^{-1} bar^{-1} day^{-1}) in TCP and Amp, respectively, and t' is time normalized such that the sinusoidal relationship has a recurring period of one year.

To assess the impact of operational set-points, summative parameters were estimated by fitting eq 3 to the time-series TCP for all combinations of TMP and passive hydraulic cleaning frequencies investigated (Figure 5). Preliminary summative parameters were estimated for each combination separately, revealing relatively similar initial TCP (319 ± 25 L m^{-2} h^{-1} bar^{-1}) and amplitude of the sinusoidal relationship (36 ± 9 L m^{-2} h^{-1} bar^{-1}) for all combinations; the average values for these were used to estimate the final summative parameters. The rates of decline in the amplitude of the sinusoidal relationship for UF1, UF2, and UF4 were observed to be similar, while the rates of decline in TCP for UF1 and UF2, as well as UF3 and UF4, were observed to be similar; the averages of these were reported as the final estimated summative parameters. A summary of the estimated summative parameters for the operational set-points investigated is presented in Table 4. Note that data for module UF3b were not considered in the present time-series analysis because this module was started much later than the others, and as a result, the biofilm in this module could not be considered to be comparable to that of the other modules. Data for UF3b is illustrated in Figure 3.

As presented in Table 4, when operating at a lower TMP (22 mbar), the frequency of passive hydraulic cleaning did not substantively impact the rate of decline in either the amplitude of the sinusoidal relationship or the overall TCP and did not have a substantive impact on the expected TCP that can be sustained over a relatively long period. However, when operating at a higher TMP (31 mbar), with less frequent passive hydraulic cleaning, the peaks and valleys in TCP were not rapidly dampened, and the expected sustained TCP was very low. Increasing the frequency of cleaning increased the dampening of the peaks and valleys in TCP and the expected sustained TCP. GDMF studies by others have also reported that a more frequent cleaning, with mechanical systems, lowered the decline in permeability.[10,46] However, regardless of the cleaning frequency, the expected TCP that can be sustained over a relatively long period was lower at a higher TMP.

The lower expected sustained TCP at a higher TMP is consistent with results from GDMF studies by others, and likely due to a greater mass transport of material to the membranes at a higher TMP and/or a higher extent of biofilm compression, leading to lower permeability.[17,18,36] The results from the present study also suggest that the frequency of passive hydraulic cleaning could be reduced when operating at

https://doi.org/10.1021/acsestwater.4c00553
ACS EST Water 2025, 5, 70−80

a lower TMP. Oka et al.[5] also reported that the frequency of hydraulic cleaning could be decreased from 24 to 48 h without impacting TCP when operating at a relatively low TMP.

A decrease in overall TCP was expected, however, as discussed in Section 3.2, the extent of the decrease was much lower than that reported in studies by others for GDMF (without hydraulic cleaning),[1,2,4,7,8,20,29−32] demonstrating the effectiveness of passive hydraulic cleaning in maintaining a higher permeability. Seasonal periods of peaks and valleys in TCP, although not expected, are not surprising given the likely impact of seasonal temperature variations on the microbial communities in the biofilm,[37,38,40] and consequently on TCP.[34−36,38,39]

The seasonal peaks and valleys in TCP dampened in the third year, likely due to the biofilm maturation over time, resulting in mostly tightly attached bacteria that are protected in the EPS layer, while loosely attached bacteria were sloughed off after each passive hydraulic cleaning.

Although operation at a lower TMP decreases the rate of decline in the overall magnitude of TCP, operation at a higher TMP and higher passive hydraulic cleaning frequency consistently generated the greatest permeate flux and, as a result, contributed the most to the total permeate flow. For this reason, all 4 membrane modules have been recently, at the end of the first 3 years of operation, set to be operated with a higher TMP (i.e., 31 mbar) and higher cleaning frequency (i.e., every 12 h). Continued monitoring is expected as part of an ongoing project.

Considering that all modules will be operating with high TMP and frequent passive hydraulic cleaning, and assuming that the past seasonal temperature variations, as well as the estimated parameters, will be representative of future conditions, using eqs 1, 2, and 3, it is possible to forecast the production flow over the years to come (Figure 2). Note that initially, changes in the production flow over time were governed by both variations in TCP and in water temperature, which influenced the viscosity and permeability of the water being filtered; however, once the variations in TCP dampened (i.e., by the end of year 3 of the present study), changes in the production flow over time are forecasted to be mainly governed by variations in water temperature.

Based on the forecasted permeate flow (Figure 2), the Klehkoot PGDMF is expected to meet the design production flow for at least another 3 years. When the production flow decreases such that it cannot meet the demand flow, the membranes will have to be replaced or chemically cleaned.

4. CONCLUSIONS

The Klehkoot PGDMF system demonstrated robust long-term performance in meeting the design production flow and regulatory water quality requirements. The system consistently met the design production flow of 10 m^3/day over the 3-year monitoring period, with the actual production flow ranging from 20 to 40 m^3/day. Regulatory water quality parameters for total coliform, *E. coli*, turbidity, and membrane integrity were consistently met.

The performance of the PGDMF system was seasonally variable, with a lower temperature-corrected permeability (TCP) associated with higher water temperatures during summer. Microbial community analysis of the feedwater revealed the greater presence of filamentous, stalked, and biofilm-forming bacteria in the summer, which likely contributed to forming a dense biofilm structure that lowered the TCP. The biofilm microbial communities were distinct from those present in the feed, permeate, and reject water, indicating the impact of unique environmental factors in shaping the biofilm.

Among the operational set-points considered, a higher TMP (i.e., 31 mbar) and higher passive hydraulic cleaning frequency (i.e., every 12 h) generated the greatest permeate flux. With these optimized parameters, the results suggest that the design production flow could be met for a total operating period of 6 years before membrane replacement or chemical cleaning is required to recover the permeability.

■ ASSOCIATED CONTENT

Supporting Information

The Supporting Information is available free of charge at https://pubs.acs.org/doi/10.1021/acsestwater.4c00553.

Additional experimental details with photographs of the membrane modules and rarefaction curves and microbiome diversity analysis results (PDF)

■ AUTHOR INFORMATION

Corresponding Author

Pierre R. Bérubé − *Department of Civil Engineering, The University of British Columbia, Vancouver, British Columbia V6T 1Z4, Canada*; Email: berube@civil.ubc.ca

Authors

Yixin Wei − *Department of Civil Engineering, The University of British Columbia, Vancouver, British Columbia V6T 1Z4, Canada*; orcid.org/0009-0000-5151-0105

Leili Abkar − *Department of Civil Engineering, The University of British Columbia, Vancouver, British Columbia V6T 1Z4, Canada*

Binura Senavirathna − *Department of Civil Engineering, The University of British Columbia, Vancouver, British Columbia V6T 1Z4, Canada*

Sara E. Beck − *Department of Civil Engineering, The University of British Columbia, Vancouver, British Columbia V6T 1Z4, Canada*; orcid.org/0000-0003-2568-0076

William Mohn − *Department of Microbiology and Immunology, The University of British Columbia, Vancouver, British Columbia V6T 1Z3, Canada*

Matt Seitcher − *Nuu-Chah-Nulth Tribal Council, Port Alberni, British Columbia V9Y 7M2, Canada*

Complete contact information is available at: https://pubs.acs.org/10.1021/acsestwater.4c00553

Notes

The authors declare no competing financial interest.

■ ACKNOWLEDGMENTS

This work was supported by Nuu-chah-nulth Tribal Council, Hupacasath First Nation, First Nation Health Authority, Indigenous Services Canada, the Natural Sciences and Engineering Research Council of Canada [NSERC Alliance Grant 558389-20], Veolia Water Technologies and Solutions, and the RES'EAU Centre for Mobilizing Knowledge.

■ REFERENCES

(1) Peter-Varbanets, M.; Hammes, F.; Vital, M.; Pronk, W. Stabilization of flux during dead-end ultra-low pressure ultrafiltration. *Water Res.* **2010**, *44* (12), 3607−3616.

(2) Peter-Varbanets, M.; Margot, J.; Traber, J.; Pronk, W. Mechanisms of membrane fouling during ultra-low pressure ultrafiltration. *J. Membr. Sci.* **2011**, *377* (1−2), 42−53.
(3) Derlon, N.; Mimoso, J.; Klein, T.; Koetzsch, S.; Morgenroth, E. Presence of biofilms on ultrafiltration membrane surfaces increases the quality of permeate produced during ultra-low pressure gravity-driven membrane filtration. *Water Res.* **2014**, *60*, 164−173.
(4) Pronk, W.; Ding, A.; Morgenroth, E.; Derlon, N.; Desmond, P.; Burkhardt, M.; Wu, B.; Fane, A. G. Gravity-driven membrane filtration for water and wastewater treatment: A review. *Water Res.* **2019**, *149*, 553−565, DOI: 10.1016/j.watres.2018.11.062.
(5) Oka, P. A.; Khadem, N.; Bérubé, P. R. Operation of passive membrane systems for drinking water treatment. *Water Res.* **2017**, *115*, 287−296.
(6) Wu, B.; Hochstrasser, F.; Akhondi, E.; Ambauen, N.; Tschirren, L.; Burkhardt, M.; Fane, A. G.; Pronk, W. Optimization of gravity-driven membrane (GDM) filtration process for seawater pretreatment. *Water Res.* **2016**, *93*, 133−140.
(7) Wu, B.; Soon, G. Q. Y.; Chong, T. H. Recycling rainwater by submerged gravity-driven membrane (GDM) reactors: Effect of hydraulic retention time and periodic backwash. *Sci. Total Environ.* **2019**, *654*, 10−18.
(8) Shi, D.; Liu, Y.; Fu, W.; Li, J.; Fang, Z.; Shao, S. A combination of membrane relaxation and shear stress significantly improve the flux of gravity-driven membrane system. *Water Res.* **2020**, *175*, No. 115694.
(9) Fortunato, L.; Ranieri, L.; Naddeo, V.; Leiknes, T. O. Fouling control in a gravity-driven membrane (GDM) bioreactor treating primary wastewater by using relaxation and/or air scouring. *J. Membr. Sci.* **2020**, *610*, No. 118261.
(10) Ranieri, L.; Vrouwenvelder, J. S.; Fortunato, L. Periodic fouling control strategies in gravity-driven membrane bioreactors (GD-MBRs): Impact on treatment performance and membrane fouling properties. *Sci. Total Environ.* **2022**, *838*, No. 156340.
(11) Peter-Varbanets, M.; Gujer, W.; Pronk, W. Intermittent operation of ultra-low pressure ultrafiltration for decentralized drinking water treatment. *Water Res.* **2012**, *46* (10), 3272−3282.
(12) Derlon, N.; Desmond, P.; Rühs, P. A.; Morgenroth, E. Cross flow frequency determines the physical structure and cohesion of membrane biofilms developed during gravity-driven membrane ultrafiltration of river water: Implication for hydraulic resistance. *J. Membr. Sci.* **2022**, *643*, No. 120079.
(13) Paul, E.; Ochoa, J. C.; Pechaud, Y.; Liu, Y.; Liné, A. Effect of shear stress and growth conditions on detachment and physical properties of biofilms. *Water Res.* **2012**, *46* (17), 5499−5508.
(14) Tang, X.; Ding, A.; Qu, F.; Jia, R.; Chang, H.; Cheng, X.; Liu, B.; Li, G.; Liang, H. Effect of operation parameters on the flux stabilization of gravity-driven membrane (GDM) filtration system for decentralized water supply. *Environ. Sci. Pollut. Res.* **2016**, *23* (16), 16771−16780.
(15) The University of British Columbia Methods and apparatus for passively bubbling gas through liquid. U.S. Patent. US0060495A1, 2021. https://patentscope.wipo.int/search/en/detail.jsf?docId=US319557300.
(16) Jain, R. Passive Membrane Filtration Systems, Ph.D. Thesis; The University of British Columbia, Dept. of Civil Engineering, 2009.
(17) Derlon, N.; Grütter, A.; Brandenberger, F.; Sutter, A.; Kuhlicke, U.; Neu, T. R.; Morgenroth, E. The composition and compression of biofilms developed on ultrafiltration membranes determine hydraulic biofilm resistance. *Water Res.* **2016**, *102*, 63−72.
(18) Desmond, P.; Morgenroth, E.; Derlon, N. Physical structure determines compression of membrane biofilms during Gravity Driven Membrane (GDM) ultrafiltration. *Water Res.* **2018**, *143*, 539−549.
(19) Jafari, M.; Derlon, N.; Desmond, P.; van Loosdrecht, M. C. M.; Morgenroth, E.; Picioreanu, C. Biofilm compressibility in ultrafiltration: A relation between biofilm morphology, mechanics and hydraulic resistance. *Water Res.* **2019**, *157*, 335−345.
(20) Wang, Q.; Tang, X.; Liang, H.; Cheng, W.; Li, G.; Zhang, Q.; Chen, J.; Chen, K.; Wang, J. Effects of Filtration Mode on the Performance of Gravity-Driven Membrane (GDM) Filtration: Cross-Flow Filtration and Dead-End Filtration. *Water* **2022**, *14* (2), No. 190.
(21) Stoffel, D.; Rigo, E.; Derlon, N.; Staaks, C.; Heijnen, M.; Morgenroth, E.; Jacquin, C. Low maintenance gravity-driven membrane filtration using hollow fibers: Effect of reducing space for biofilm growth and control strategies on permeate flux. *Sci. Total Environ.* **2022**, *811*, No. 152307.
(22) Indian & Northern Affairs Canada (INAC) Protocol for Centralised Drinking Water Systems in First Nations Communities, 2024. https://www.sac-isc.gc.ca/eng/1100100034998/1533666593873. (accessed February 10, 2024).
(23) Standard Methods for the Examination of Water and Wastewater. In *American Public Health Association (APHA)*, 23rd ed.; Baird, R. B.; Eaton, A. D.; Rice, E. W., Eds.; American Water Works Association: Washington D.C., 2017.
(24) Abkar, L.; Taylor, A.; Stoddart, A.; Gagnon, G. Microbiome and hydraulic performance changes of drinking water biofilters during disruptive events-media replacement, lake diatom bloom, and chlorination. *Environ. Sci.: Water Res. Technol.* **2023**, *9* (3), 723−735.
(25) Langille Lab Amplicon-SOP-v2-(qiime2−2018.6), 2024. https://github.com/LangilleLab/microbiome_helper/wiki/. (accessed April 24, 2024).
(26) QIIME 2 Data Resources—Taxonomy Classifiers for Use with q2-Feature-Classifier 2023. https://docs.qiime2.org/2023.9/data-resources/. (accessed April 24, 2024).
(27) US EPA Membrane Filtration Guidance Manual. Long Term 2 Enhanced Surface Water Treatment Rule Documents, 2024. https://www.epa.gov/dwreginfo/long-term-2-enhanced-surface-water-treatment-rule-documents. (accessed January 10, 2024).
(28) Health Canada Guidelines for Canadian Drinking Water Quality—Summary Tables, 2024. https://www.canada.ca/en/health-canada/services/environmental-workplace-health/reports-publications/water-quality/guidelines-canadian-drinking-water-quality-summary-table.html. (accessed January 10, 2024).
(29) Shao, S.; Shi, D.; Li, Y.; Liu, Y.; Lu, Z.; Fang, Z.; Liang, H. Effects of water temperature and light intensity on the performance of gravity-driven membrane system. *Chemosphere* **2019**, *216*, 324−330.
(30) Stoffel, D.; Derlon, N.; Traber, J.; Staaks, C.; Heijnen, M.; Morgenroth, E.; Jacquin, C. Gravity-driven membrane filtration with compact second-life modules daily backwashed: An alternative to conventional ultrafiltration for centralized facilities. *Water Res. X* **2023**, *18*, No. 100178.
(31) Lee, D.; Baek, Y.; Son, H.; Chae, S.; Lee, Y. Pre-ozonation for gravity-driven membrane filtration: Effects of ozone dosage and application timing on membrane flux and water quality. *Chem. Eng. J.* **2023**, *473*, No. 145160.
(32) Lee, D.; Lee, Y.; Choi, S. S.; Lee, S. H.; Kim, K. W.; Lee, Y. Effect of membrane property and feed water organic matter quality on long-term performance of the gravity-driven membrane filtration process. *Environ. Sci. Pollut. Res.* **2019**, *26* (2), 1152−1162.
(33) Desmond, P.; Best, J. P.; Morgenroth, E.; Derlon, N. Linking composition of extracellular polymeric substances (EPS) to the physical structure and hydraulic resistance of membrane biofilms. *Water Res.* **2018**, *132*, 211−221.
(34) Lin, L.; Zhang, Y.; Yan, W.; Fan, B.; Fu, Q.; Li, S. Performance of gravity-driven membrane systems for algal water treatment: Effects of temperature and membrane properties. *Sci. Total Environ.* **2022**, *838*, No. 155963.
(35) Shami, I. U. H.; Wu, B. Gravity-driven membrane reactor for decentralized wastewater treatment: Effect of reactor configuration and cleaning protocol. *Membranes* **2021**, *11* (6), No. 388.
(36) Akhondi, E.; Wu, B.; Sun, S.; Marxer, B.; Lim, W.; Gu, J.; Liu, L.; Burkhardt, M.; McDougald, D.; Pronk, W.; Fane, A. G. Gravity-driven membrane filtration as pretreatment for seawater reverse osmosis: Linking biofouling layer morphology with flux stabilization. *Water Res.* **2015**, *70*, 158−173.

(37) Liu, H.; Zhu, L.; Tian, X.; Yin, Y. Seasonal variation of bacterial community in biological aerated filter for ammonia removal in drinking water treatment. *Water Res.* **2017**, *123*, 668−677.
(38) Tao, C.; Parker, W.; Bérubé, P. Characterization and modelling of soluble microbial products in activated sludge systems treating municipal wastewater with special emphasis on temperature effect. *Sci. Total Environ.* **2021**, *779*, No. 146471.
(39) Ma, Z.; Wen, X.; Zhao, F.; Xia, Y.; Huang, X.; Waite, D.; Guan, J. Effect of temperature variation on membrane fouling and microbial community structure in membrane bioreactor. *Bioresour. Technol.* **2013**, *133*, 462−468.
(40) Ma, B.; LaPara, T. M.; Hozalski, R. M. Microbiome of Drinking Water Biofilters is Influenced by Environmental Factors and Engineering Decisions but has Little Influence on the Microbiome of the Filtrate. *Environ. Sci. Technol.* **2020**, *54* (18), 11526−11535.
(41) Wu, Z.; Ye, C.; Guo, F.; Zhang, S.; Yu, X. Evidence for broad-spectrum biofilm inhibition by the bacterium Bacillus sp. strain SW9. *Appl. Environ. Microbiol.* **2013**, *79* (5), 1735−1738.
(42) Shivaji, S.; Nagapriya, B.; Ranjith, K. Differential Susceptibility of Mixed Polymicrobial Biofilms Involving Ocular Coccoid Bacteria (Staphylococcus aureus and S. epidermidis) and a Filamentous Fungus (Fusarium solani) on Ex Vivo Human Corneas. *Microorganisms* **2023**, *11* (2), No. 413.
(43) Jackson, C. R.; Churchill, P. F.; Roden, E. E. Successional changes in bacterial assemblage structure during epilithic biofilm development. *Ecology* **2001**, *82* (2), 555−566.
(44) Besemer, K.; Peter, H.; Logue, J. B.; Langenheder, S.; Lindström, E. S.; Tranvik, L. J.; Battin, T. J. Unraveling assembly of stream biofilm communities. *ISME J.* **2012**, *6* (8), 1459−1468.
(45) Henne, K.; Kahlisch, L.; Brettar, I.; Höfle, M. G. Analysis of structure and composition of bacterial core communities in mature drinking water biofilms and bulk water of a citywide network in Germany. *Appl. Environ. Microbiol.* **2012**, *78* (10), 3530−3538.
(46) Lee, S.; Sutter, M.; Burkhardt, M.; Wu, B.; Chong, T. H. Biocarriers facilitated gravity-driven membrane (GDM) reactor for wastewater reclamation: Effect of intermittent aeration cycle. *Sci. Total Environ.* **2019**, *694*, No. 133719.

https://doi.org/10.1021/acsestwater.4c00553
ACS EST Water 2025, 5, 70−80